AIP | Physics of Fluids

The effects of capillary forces on the axisymmetric propagation of two-phase, constant-flux gravity currents in porous media

Madeleine J. Golding, Herbert E. Huppert, and Jerome A. Neufeld

Citation: Phys. Fluids **25**, 036602 (2013); doi: 10.1063/1.4793748
View online: http://dx.doi.org/10.1063/1.4793748
View Table of Contents: http://pof.aip.org/resource/1/PHFLE6/v25/i3
Published by the American Institute of Physics.

PHYSICS OF FLUIDS **25**, 036602 (2013)

The effects of capillary forces on the axisymmetric propagation of two-phase, constant-flux gravity currents in porous media

Madeleine J. Golding,[1,a)] Herbert E. Huppert,[1,2] and Jerome A. Neufeld[1,3,4]
[1]*Department of Applied Mathematics and Theoretical Physics, Institute of Theoretical Geophysics, University of Cambridge, Cambridge CB3 0WA, United Kingdom*
[2]*School of Mathematics, University of New South Wales, Kensington, NSW 2052, Australia and Faculty of Science, University of Bristol, Bristol BS2 6BB, United Kingdom*
[3]*BP Institute, Bullard Laboratories, University of Cambridge, Madingley Road, Cambridge CB3 0EZ, United Kingdom*
[4]*Bullard Laboratories, Department of Earth Sciences, University of Cambridge, Madingley Road, Cambridge CB3 0EZ, United Kingdom*

(Received 13 July 2012; accepted 20 December 2012; published online 21 March 2013)

The effects of capillary forces on the propagation of two-phase, constant-flux gravity currents in a porous medium are studied analytically and numerically in an axisymmetric geometry. The fluid within a two-phase current generally only partially saturates the pore space it invades. For long, thin currents, the saturation distribution is set by the vertical balance between gravitational and capillary forces. The capillary pressure and relative permeability of the fluid in the current depend on this saturation. The action of capillary forces reduces the average saturation, thereby decreasing the relative permeability throughout the current. This results in a thicker current, which provides a steeper gradient to drive flow, and a more blunt-nose profile. The relative strength of gravity and capillary forces remains constant within a two-phase gravity current fed by a constant flux and spreading radially, due to mass conservation. For this reason, we use an axisymmetric representation of the framework developed by Golding *et al.* ["Two-phase gravity currents in porous media," J. Fluid Mech. **678**, 248–270 (2011)], to investigate the effect on propagation of varying the magnitude of capillary forces and the pore-size distribution. Scaling analysis indicates that axisymmetric two-phase gravity currents fed by a constant flux propagate like $t^{1/2}$, similar to their single-phase counterparts [S. Lyle, H. E. Huppert, M. Hallworth, M. Bickle, and A. Chadwick, "Axisymmetric gravity currents in a porous medium," J. Fluid Mech. **543**, 293–302 (2005)], with the effects of capillary forces encapsulated in the constant of proportionality. As a practical application of our new concepts and quantitative evaluations, we discuss the implications of our results for the process of carbon dioxide (CO_2) sequestration, during which gravity currents consisting of supercritical CO_2 propagate in rock saturated with aqueous brine. We apply our two-phase model including capillary forces to quantitatively assess seismic images of CO_2 spreading at Sleipner underneath the North Sea. © *2013 American Institute of Physics*. [http://dx.doi.org/10.1063/1.4793748]

I. INTRODUCTION

Gravity currents in porous media occur in many natural and industrial settings, wherever gravity acting vertically on the density difference between fluids drives mainly horizontal propagation. When the propagating and ambient fluids are immiscible, the action of capillary forces results in a region occupied by both phases called the transition zone or capillary fringe. Capillary forces also cause

a)M.J.Golding@damtp.cam.ac.uk.

residual trapping, where one of the phases becomes trapped as the gravity current propagates. Examples of two-phase gravity currents include the spread of pollutants below the water table, the migration of oil and natural gas in the subsurface, and groundwater spreading along the lower boundary of a perched reservoir. The thickness of this transition zone depends on the strength of the capillary forces acting within the current and the geometry of the porous medium. This contrasts with single-phase currents where capillary forces are absent or negligible and the fluid in the current fully saturates the pores, thus leading to a clear interface between the intruding and ambient fluids. An example of a single-phase gravity current is the intrusion of dense saltwater into an underground freshwater reservoir.

One particularly timely example of a situation where two-phase gravity currents occur is the geological sequestration of CO_2. Here, capillary forces between buoyant CO_2 and relatively dense brine serve to create a capillary fringe of partial CO_2 saturation. It is important to understand how two-phase effects alter the propagation of such gravity currents and how much thicker the current becomes. Thicker currents contact a greater region of the reservoir, which affects the storage potential of reservoirs. Furthermore, it is not clear *a priori* how two-phase effects alter either the speed of propagation or horizontal extent of a two-phase gravity current. The volume of rock reached by CO_2, along with the saturation distribution of CO_2 within it, has important implications for the amount of CO_2 that can be permanently immobilised by way of residual trapping.

Capillary forces acting within a two-phase gravity current result in partial saturation of the intruding fluid within pore spaces. This decreases the pore space available to the intruding fluid, thus reducing the relative permeability. Capillary forces acting alongside gravity cause the saturation distribution to be non-uniform with depth, leading to a variation of relative permeability within the current. The relative strength of capillary and buoyancy forces within the current is set by the rate of increase of fluid in the current (e.g., constant flux or finite volume), as well as the geometry of the current (e.g., two-dimensional or radial).

Gravity currents have traditionally been studied using sharp-interface models, where each fluid fully saturates the pore space it occupies and there is a sharp boundary between the injected and ambient fluids. The axisymmetric spreading of gravity currents along horizontal boundaries in porous media was studied by Lyle *et al.*[1] and the effect of sloping boundaries on initially axisymmetric gravity currents was investigated by Vella and Huppert.[2] Such models are appropriate for two-phase gravity currents when capillary forces are negligible, but not when a significant transition zone exists.

Previous sharp-interface, or uniform-saturation, models include residual trapping by assuming that a constant proportion of the fluid is trapped. Kochina, Mikhailov, and Filinov[3] studied a slumping groundwater mound, Hesse, Orr, Jr., and Tchelepi[4] considered the spreading of a finite volume of CO_2 in a confined aquifer, and Juanes, MacMinn, and Szulczewski[5] investigated the efficiency of residual trapping in the wake of a CO_2 plume. These models attempt to approximately capture only the dependence of the volume of trapped fluid on the volume of rock the current invades. However, they are unable to account for the extra thickness of the current, or the effect of variations in saturation within the current, caused by capillary forces.

Examples of multiphase models for three-phase, gravity-driven systems include those presented by Bear and Ryzhik[6] and by Blunt, Zhou, and Fenwick,[7] which were motivated by non-aqueous phases, such as chemical spills, and Yortsos,[8] who was motivated by oil recovery. Philip[9] used the classical two-phase flow equations to study the evolution of water saturation within unsaturated soil in situations where gravity either can be neglected or does not significantly alter the aspect ratio of the fluid flow. More recently, two-phase models have been developed to understand CO_2 sequestration. For example, Nordbotten and Dahle[10] have developed a vertically integrated model for two-phase gravity currents in a confined aquifer. A framework for investigating two-dimensional two-phase gravity currents in unconfined aquifers was developed by Golding *et al.*,[11] in which an explicit expression for the saturation distribution was obtained from the vertical balance between gravitational and capillary forces, commonly referred to as vertical gravity-capillary equilibrium. The model therefore resolves the non-uniform saturation distribution and incorporates the resultant structure of the relative permeabilities into predictions for the propagation of buoyancy-driven currents. This is particularly important if the current contains non-wetting fluid because the amount

of fluid subsequently trapped once injection ceases is known to depend on the maximum saturation during its initial emplacement.[12] A quantitative estimation of these effects is of particular interest in CO_2 sequestration, where residual trapping is widely regarded as one of the most promising mechanisms for permanently immobilizing CO_2 in the storage site.

Golding *et al.*[11] employed their framework to evaluate the effects of capillary forces within a steady-state, two-dimensional gravity current spreading over a finite, horizontal barrier. Application of the model to propagating two-dimensional gravity currents over an infinite impermeable boundary is of limited interest because gravitational forces always become dominant as the height of the current increases, causing the behaviour of the current to tend to the single-phase limit. In contrast, mass conservation in axisymmetric gravity currents fed by a constant flux, both single-phase and two-phase, results in the height scale of the current remaining constant with time, and hence the relative strength of capillary and gravity forces is fixed. Thus the consideration of axisymmetric spreading in this study enables us to investigate the effects of two-phase phenomena on the propagation of two-phase gravity currents over a semi-infinite, impermeable horizontal boundary. Under the assumption of gravity-capillary equilibrium, which is valid throughout all but the nose of the gravity current, our framework is able to resolve the vertical saturation distribution within the current and recovers the attractive analytical results by Lyle *et al.*[1] in the appropriate limit of negligible capillary forces.

In this paper we show how capillary forces can be included in models of the structure and propagation of axisymmetric, unconfined gravity currents in porous media. The equations governing the height of a propagating axisymmetric two-phase gravity current are derived in Sec. II and are based on the two-dimensional model developed by Golding *et al.*[11] We find a self-similar solution to these equations in Sec. III with the aid of scaling analysis. The effect of capillarity on the shape and propagation rate of two-phase gravity currents is investigated in Sec. IV, as well as the sensitivity of the behaviour to the main two-phase parameters. Finally in Sec. V, we discuss the results and their implications for modeling gravity currents during CO_2 sequestration.

II. THE AXISYMMETRIC TWO-PHASE GRAVITY CURRENT MODEL

We consider the buoyancy-driven propagation of an axisymmetric gravity current, fed by a constant flux of non-wetting fluid, in a porous medium fully saturated with an immiscible fluid of larger density and different viscosity as shown in Figure 1. This process, where a non-wetting fluid invades a porous medium fully saturated with a wetting fluid, is known as primary drainage, as is the case for CO_2 sequestration. However, we note that the results are general and apply equally to the case of injected wetting fluid, which would be a primary imbibition process. Furthermore, the theory is also applicable when the injected fluid is denser than the ambient fluid and the gravity current propagates above a horizontal boundary. In all cases, the pressure gradients in the ambient fluid are negligible far from the current in an unconfined aquifer. Given the assumption that the ambient fluid remains fully connected everywhere in the region, we can imply that there are no horizontal pressure gradients driving the wetting fluid anywhere, including within the gravity current. The axisymmetric gravity current model is based on and extends the two-dimensional equivalent derived

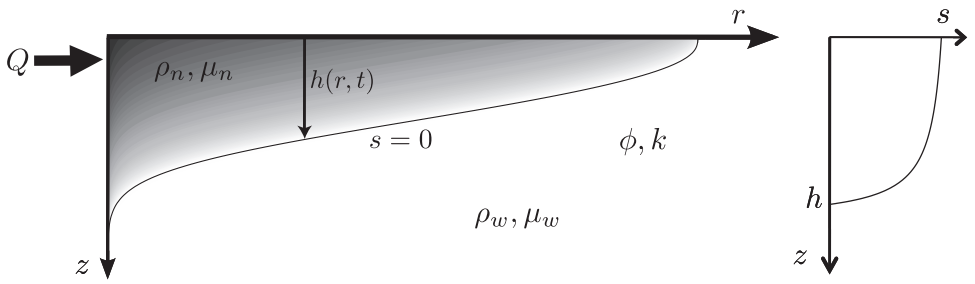

FIG. 1. (Left) A sketch of an axisymmetric gravity current propagating below an impermeable horizontal boundary in a porous medium saturated with an immiscible fluid of higher density and different viscosity. (Right) A representative vertical saturation profile through the current, as indicated by the gray shading on the left.

in Golding *et al.*[11] Here we briefly review the two-phase theory as needed for the development in this paper. We denote quantities pertaining to the non-wetting and wetting phases by subscripts n and w, respectively.

The motion of two phases in a porous medium is governed by local mass conservation,

$$\phi \frac{\partial S_i}{\partial t} + \nabla \cdot \mathbf{u}_i = 0 \qquad (i = n, w), \tag{1}$$

where ϕ is the porosity of the porous medium, $\mathbf{u}_i$ is the volumetric flux of phase i, and S_i is the fraction of pore space occupied by phase i, and therefore

$$S_n + S_w = 1. \tag{2}$$

During drainage, a fraction of the wetting phase remains within the pore space and is known as the irreducible wetting phase saturation, S_{wi}. An effective non-wetting phase saturation can therefore be defined as

$$s = S_n/(1 - S_{wi}). \tag{3}$$

When immiscible fluids coexist within the same pore space, the interfacial tension between them causes a difference in pressure between the phases, known as the capillary pressure

$$p_c(s) = p_n - p_w. \tag{4}$$

The capillary pressure is assumed to be a function of saturation only. One commonly used empirical constitutive relation is Brooks-Corey

$$p_c = p_e(1 - s)^{-1/\Lambda} \tag{5a}$$

or

$$s = 1 - (p_c/p_e)^{-\Lambda}, \tag{5b}$$

where the parameters Λ and p_e are determined experimentally,[13] but can be physically interpreted as follows. At the pore-scale a capillary pressure threshold must be overcome for the non-wetting phase to enter pores during drainage. This capillary entry pressure for each pore is inversely proportional to the size of its throat, so the non-wetting phase preferentially fills larger pores, whereas the wetting phase fills the smaller pores first. The parameter p_e can therefore be interpreted as the entry pressure required for the non-wetting phase to enter the largest pores. As the pressure is increased, the non-wetting fluid invades successively smaller pores whose distribution is captured by the parameter Λ. A narrow pore-size distribution, corresponding to a large value of Λ, results in a rapid increase in saturation with pressure because all the pores in the porous medium have a similar capillary entry pressure. This results in a narrow transition zone and consequently capillary effects are weak. Alternatively, for a wider pore-size distribution, where Λ is smaller, each increase in pressure causes invasion of only a small number of slightly smaller pores. This results in a broad transition zone and enhances capillary effects.

The volumetric flux of phase i is given by a two-phase Darcy's law

$$\mathbf{u}_i = -\frac{k k_{ri}(s)}{\mu_i} [\nabla p_i - \rho_i \mathbf{g}] \qquad i = n, w, \tag{6}$$

where k is the intrinsic permeability of the porous medium, which we assume is homogeneous, $\mathbf{g}$ is the gravitational acceleration, ρ_i and μ_i are the density and dynamic viscosity of phase i, respectively, and p_i is the averaged pressure within phase i. The relative permeability of each phase, $k_{ri}(s)$, is itself a unique nonlinear function of the saturation during primary drainage for a given system of fluids and porous medium, which can only be fully determined empirically. Wetting effects influence the size of the pores occupied by each phase, which implies that relative permeability must depend on the pore-size distribution. Several models have been developed to obtain full relative permeability curves from capillary pressure measurements, which capture the effects of the pore-size distribution. Brooks and Corey[14] used their expression for capillary pressure (5) to obtain explicit expressions

for the relative permeability of the non-wetting and wetting phases, and expressed them as

$$k_{rn} = k_{rn0} s^2 [1 - (1 - s)^{(2+\Lambda)/\Lambda}] \tag{7a}$$

and

$$k_{rw} = (1 - s)^{(2+3\Lambda)/\Lambda}, \tag{7b}$$

respectively, where the end point relative permeability of the non-wetting phase, k_{rn0}, is determined empirically. Li and Horne[15] review a range of these models, assess their validity in various two-phase systems, and find that the Brooks-Corey relative permeability model works well in drainage cases.

In this study we consider the propagation of a long, thin gravity current for which the vertical velocity of each phase is negligible compared to the horizontal velocity of the non-wetting fluid within the current. Therefore, assuming the fluids are fully connected, the pressure within each phase is approximately hydrostatic and so (4) can be written as a function of vertical position, z, as

$$p_c[h(r, t), z] = p_e - \Delta\rho g(z - h), \tag{8}$$

where $\Delta\rho = \rho_w - \rho_n$. Here, we have used the assumption that p_e is the value of the capillary pressure at the current boundary, $z = h$, where the non-wetting phase saturation is zero. Golding *et al.*[11] derived an expression for the saturation distribution within a long, thin gravity current by substituting the Brooks-Corey capillary pressure model (5) into the expression for gravity-capillary equilibrium (8) to obtain

$$s[h(r, t), z] = 1 - \left(1 + \frac{h - z}{h_e}\right)^{-\Lambda}, \tag{9}$$

where

$$h_e \equiv p_e / \Delta\rho g \tag{10}$$

is an approximate length scale over which the hydrostatic pressure exceeds p_e. This determines the saturation, as a function of depth, within a propagating two-phase current, assumed to be in gravity-capillary equilibrium. The validity of this assumption is discussed at the end of this section. In this two-phase model, the saturation tends to $s = 1$ asymptotically when the capillary pressure tends to infinity, as expressed by the Brooks-Corey capillary pressure curve (5). However, when capillary effects are very weak, the saturation can be approximated by $s \approx 1$ in the majority of the current.

In order to find the evolution equation for the height of the gravity current, we vertically integrate (1) for the non-wetting phase between 0 and h, and for an axisymmetric geometry find that

$$\varphi s_0(h/h_e)\frac{\partial h}{\partial t} - u_b \frac{1}{r}\frac{\partial}{\partial r}\left[rh\frac{\partial h}{\partial r}\mathcal{F}(h/h_e)\right] = 0, \tag{11}$$

where $\varphi = \phi(1 - S_{wi})$ is an effective porosity which accounts for the irreducible wetting phase saturation, $u_b = \Delta\rho g k k_{rn0}/\mu_n$ is the buoyancy velocity, and k_{rn0} is the non-wetting phase relative permeability at the maximum end-point saturation, $s = 1$. A more detailed explanation of this step, which also uses the condition of zero saturation at $z = h$, is presented by Golding *et al.*[11] Two-phase effects are incorporated by the inclusion of a saturation function

$$s_0(h/h_e) = 1 - \left(1 + \frac{h}{h_e}\right)^{-\Lambda}, \tag{12}$$

and a flux function

$$\mathcal{F}(h/h_e) \equiv \frac{1}{k_{rn0}h}\int_0^h k_{rn}[s(z)]dz \tag{13}$$

$$= \frac{h_e}{\Lambda h}\int_0^{s_0(h/h_e)} s^2\left[(1 - s)^{-(\Lambda+1)/\Lambda} - (1 - s)^{1/\Lambda}\right]ds, \tag{14}$$

where we have used (9) to change variables and (7a) for the relative permeability. This two-phase model for the propagation of axisymmetric, porous gravity currents reduces to the single-phase model when $S_{wi} \equiv 0$, $k_{rn0} \equiv 1$, and in the limit $s(h, z) \equiv 1$, $s_0(h/h_e) \equiv 1$, and $\mathcal{F}(h/h_e) \equiv 1$.

We note that the saturation and flux functions, (12) and (13), remain unchanged between two-dimensional propagation, presented in Golding *et al.*,[11] and radial spreading, presented here, as they incorporate only the vertical balance between gravity and capillarity. Here we are using a different relative permeability model from the power law used by Golding *et al.*,[11] who assumed that $k_{rn} = k_{rn0}s^{\alpha}$, where α is an empirically obtained constant. This is in order to more easily and consistently capture and illustrate the effect of pore-size distribution, described by Λ, on relative permeability.

The edge of the current is located at $r_N(t)$, at which point

$$h[r_N(t), t] = 0. \tag{15}$$

Global conservation of the mass of non-wetting fluid is given by

$$2\pi\varphi \int_0^{r_N(t)} \int_0^{h(r,t)} s[h(r,t), z] r dz dr = Qt, \tag{16}$$

where Q is the constant volumetric flux of non-wetting fluid into the current.

Equivalently, the flux through the nose of the current is zero, so

$$\left[rh \frac{\partial h}{\partial r} \mathcal{F}(h/h_e) \right]_{r=r_N} = 0, \tag{17}$$

and the flux at the origin is given by

$$-2\pi u_b \left[rh \frac{\partial h}{\partial r} \mathcal{F}(h/h_e) \right]_{r\to 0} = Q. \tag{18}$$

These expressions can be obtained by integrating (11) with respect to r and substituting it into (16) differentiated with respect to t.

It is clear from (18) that near the injection point at $r = 0$, $\partial h/\partial r$ must tend to infinity to maintain a constant flux, and hence the assumption of negligible vertical velocity required for gravity-capillary equilibrium is not valid there. We acknowledge that this model therefore does not capture the height profile of the current in this region, but as with all vertical equilibrium models, assume that the fluid very quickly transitions to the gravity-capillary equilibrium regime at radii beyond where the height has dropped near the source. For example, Huppert[16] verified experimentally that the very localised regions near the origin, and the nose, do not have a significant effect on the remainder of axisymmetric, viscous gravity currents.

III. SELF-SIMILAR PROPAGATION OF TWO-PHASE GRAVITY CURRENTS

The formalism developed in Sec. II provides the necessary tools to assess the effect of capillary forces on the buoyancy-driven propagation of immiscible currents within porous media and could be used to study many different situations. Here we consider the specific problem of the axisymmetric spreading of the non-wetting fluid along a horizontal impermeable barrier from a source of constant flux. The aim is to understand how capillary forces affect the motion and profile of the current over time. It is also important to find how the saturation distribution within the current evolves, because this has important consequences on the residual trapping that occurs once injection has ceased.

Scaling analysis of (11) and (16) indicates that

$$r \sim (Qu_b/\varphi^2)^{1/4} (\mathcal{F}/s_0^2)^{1/4} t^{1/2} \tag{19a}$$

and

$$h \sim (Q/u_b)^{1/2} \mathcal{F}^{-1/2}. \tag{19b}$$

We immediately see that, as in the single-phase case, the two-phase current height has no explicit time dependence. Therefore the dimensionless functions s_0 and $\mathcal{F}$, which depend only on h, have no explicit time dependence and it follows from (19a) that the radius of the current $r_N(t) \propto t^{1/2}$. A central and somewhat surprising result of our study is therefore that, in the geometry investigated, two-phase axisymmetric gravity currents propagate with the same $t^{1/2}$ spreading rate found for single-phase

currents.[1] This scaling of radius with $t^{1/2}$ is also found in the confined case[10] for the same reason of mass conservation. Furthermore in this unconfined case, the lack of an external length scale in the problem indicates a self-similar solution for the spreading currents, which we have verified is consistent with the results from the numerical solution of (11) to (16). Capillary forces modify both the speed, as given by the prefactor in the spreading, and the profile of spreading currents, as shown below. We see also from (19a) and (19b) that the aspect ratio of the current $r/h \sim t^{1/2}$, which implies that after sufficient time the gravity current is always long and thin, and the assumption of vertical equilibrium is valid.

Motivated by (19a) and (19b), we look for solutions as a function of the similarity variable

$$\eta = \left(\varphi^2/Qu_b\right)^{1/4} rt^{-1/2}, \tag{20}$$

such that the radius of the current is given by

$$r_N(t) = \eta_N (Qu_b/\varphi^2)^{1/4} t^{1/2}, \tag{21}$$

where η_N is a constant to be determined for a given set of parameter values. Relation (19a) indicates that

$$\eta_N \sim \left(\mathcal{F}/s_0^2\right)^{1/4}, \tag{22}$$

where s_0 and $\mathcal{F}$ are evaluated at some representative value of height h. Hence it is the multiplicative factor η_N that incorporates the effects of capillary forces on the propagation rate of a two-phase gravity current.

The profile of the current is given by

$$h = Hf(y), \tag{23}$$

where the vertical scale

$$H = (Q/u_b)^{1/2}, \tag{24}$$

and the dimensionless height profile f is solely a function of y, the scaled similarity variable, defined as

$$y \equiv \eta/\eta_N. \tag{25}$$

From (19b) we see that

$$f\mathcal{F}(f)^{1/2} \sim 1. \tag{26}$$

We introduce a Bond number, which is the ratio of gravitational to capillary forces,

$$B \equiv \Delta\rho g H/p_e = H/h_e, \tag{27}$$

in an analogous manner to Golding *et al.*,[11] and note that the vertical scale of the current is independent of time for a constant-flux, axisymmetric, two-phase gravity current. The relative strength of gravity and capillary forces therefore does not change as the gravity current propagates, as characterised by a constant Bond number. This is an ideal situation in which to investigate two-phase effects on propagating gravity currents and is the reason for choosing an axisymmetric geometry with a constant input flux. This situation is in contrast with two-dimensional gravity currents fed by a constant or increasing flux, or indeed axisymmetric gravity currents whose flux increases with time. In all of these cases, the height and therefore Bond number increase with time. Hence, regardless of initial conditions, the behaviour of the gravity current tends towards the single-phase limit modeled by Huppert and Woods[17] and Lyle *et al.*[1] for the two-dimensional and axisymmetric geometries, respectively.

The equation governing the similarity solution for the current height, f, is obtained by changing variables from (r, t) to y using (20) in (11), and substituting (23) into the result, which yields

$$\left[yff'\mathcal{F}(fB)\right]' + \frac{1}{2}\eta_N^2 y^2 f' s_0(fB) = 0, \tag{28}$$

where a prime denotes d/dy. The boundary conditions are now

$$f(y=1)=0 \tag{29}$$

and

$$\eta_N = \left[2\pi \int_0^1 \int_0^f s[Bf(y),z]ydzdy\right]^{-1/2}, \tag{30}$$

which define the nose and enforce global mass conservation, respectively.

The saturation and flux functions become

$$s_0(fB) = 1-(1+fB)^{-\Lambda} \tag{31}$$

and

$$\mathcal{F}(fB) = \frac{1}{\Lambda fB}\int_0^{s_0(fB)} s^2\left[(1-s)^{-(\Lambda+1)/\Lambda}-(1-s)^{1/\Lambda}\right]ds. \tag{32}$$

The analytical expression obtained by integrating (32), not explicitly needed here, is displayed in the Appendix. The limiting physical behaviour of the saturation and flux functions are discussed further in Sec. IV.

Equation (28) along with conditions (29) and (30) and the specific models for the saturation (31) and flux function (32) provides a closed model for the profile and propagation of the two-phase axisymmetric gravity current. In order to calculate the dimensionless height profile, f, and determine the value of the similarity variable at the current front, η_N, we solve (28) numerically, together with (29) and (30). To obtain the third and final condition required to solve the problem, we approximate the saturation and flux functions at the nose, where $fB \ll 1$, by

$$s_0(fB) \approx \Lambda Bf \tag{33a}$$

and

$$\mathcal{F}(fB) \approx \frac{\Lambda^2}{4}(2+\Lambda)(fB)^3, \tag{33b}$$

and seek a solution of (28) of the form $f(y) = p(1-y)^q$. This yields the gradient condition at the current nose, given by

$$f' = -\frac{1}{3}\left[\frac{3\eta_N^2}{\Lambda(2+\Lambda)B^2}\right]^{1/3}(1-y)^{-2/3} \qquad (1-y \ll 1). \tag{34}$$

In general, both η_N and $f(y)$ are functions of Λ and B. However, it is possible to make approximations to the equations in certain limits, which we demonstrate in Sec. IV in order to obtain analytical expressions for the behaviour of the current. In the case of either very weak or very strong capillary forces, the problem greatly simplifies to become independent of Λ and B, apart from a simple scaling in the latter case. We find that when $fB \gg 1$ and $\Lambda \ll 1$, the number of parameters controlling η_N and the height profile $f(y)$ is reduced, thereby simplifying the problem.

IV. TWO-PHASE EFFECTS ON SELF-SIMILAR CURRENTS

The action of capillary forces within two-phase gravity currents results in a region of partial saturation, known as the transition zone, or capillary fringe. The saturation determines the volume of each fluid contained locally in the pores and its relative permeability, both of which control the shape and propagation of two-phase currents. It is the balance between gravity and capillary forces that determines the saturation distribution as a function of the vertical position within a current as expressed by (8).

The strength of capillary forces determines the width of the capillary fringe relative to the depth of the current, which is therefore a measure of the influence of capillary forces on the behaviour of the two-phase current. When capillary forces are relatively small, the capillary fringe is negligible, $s \approx 1$ in most of the current, and the behaviour approaches the single-phase limit. Conversely, when capillary forces are large, the capillary fringe is wide and the average saturation, and hence relative

permeability, within the current is lower. In such currents capillary forces can have a strong influence on the shape and velocity of propagation.

The height of the current compared to the capillary entry height defined by (10) is characterized by $fB = h/h_e = \Delta\rho g h/p_e = [p_c(h, z = 0) - p_e]/p_e$, where (8) is used in the last equality and is equivalent to the change in capillary pressure across the vertical extent of the current divided by the capillary entry pressure. It is therefore a measure of the relative strength of gravitational to capillary forces. The vertical saturation gradient associated with a given height or pressure difference is determined by the pore-size distribution, Λ. A narrow pore-size distribution, $\Lambda \gg 1$, leads to a sharp increase in non-wetting phase saturation over a small distance, whereas a wide pore-size distribution, $\Lambda \ll 1$, leads to a more gradual change of saturation with height. Thus, the size of the capillary fringe in comparison to the current height depends on both the Bond number and the pore-size distribution.

The parameter Λ is used to fit the Brooks-Corey model for the relation between capillary pressure and saturation to empirical data. It indicates the distribution of pore sizes within a porous medium and can therefore take a wide range of values in a multitude of industrial, laboratory, and geophysical settings. Examples of typical values found in the literature are 2/3 for a reservoir sandstone, discussed in Sec. V, 0.4 for water and air in a mixture of bentonite and crushed rock,[18] and 3.7 for water and air in fine sand.[13] As the pore-size distribution becomes narrower, for example, in a sand pack in a laboratory experiment where all the sand particles are of the same size, the value of Λ increases towards its limit of ∞, which indicates a porous medium of uniform pore size. The value of B depends on many parameters describing the input flux, fluids, and porous medium, all of which themselves depend on factors such as temperature and pressure, and can vary greatly depending on the physical system.[19] In this section we therefore consider a wide range of parameter values for B and Λ to fully explore how capillary forces affect two-phase gravity currents.

The effects of capillary forces on the behaviour of two-phase gravity currents are incorporated in the model by the saturation and flux functions. Contour plots of s_0 and $\mathcal{F}$ are displayed in Figure 2 and show how these two functions depend on the relative strength of capillary forces, characterized by fB, and the pore-size distribution, characterized by Λ. There are three physical limits, shaded gray, where the constitutive saturation and flux functions display distinct behaviour according to the strength of capillary forces acting in the pore geometry compared to gravity. These regions correspond to: (1) weak capillary forces (large fB, large Λ); (2) strong capillary forces (small fB, acting in a range of pore-size distributions Λ); and (3) weak to intermediate capillary forces (large fB, acting in a wide pore-size distribution, small Λ, which magnifies capillary effects). Approximate expressions for s_0 and $\mathcal{F}$ can be found in these limits, as described in Secs. IV A–IV C, and are plotted using dashed curves in regions 2 and 3 in Figure 2.

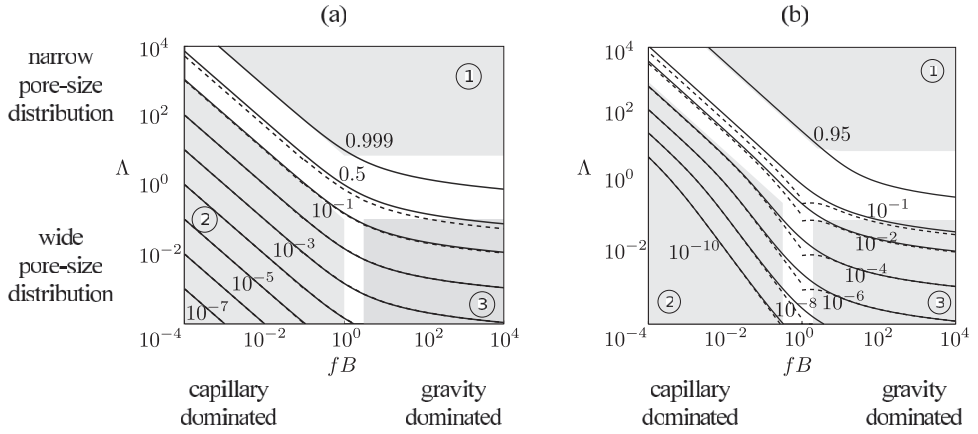

FIG. 2. Contour plots of (a) the saturation function, s_0, and (b) the flux function, $\mathcal{F}$, against fB and Λ. The shaded regions indicate the physical limits of (1) weak, (2) strong, and (3) intermediate capillary effects discussed in Secs. IV A–IV C, respectively, as well as the regions for which approximate expressions for s_0 and $\mathcal{F}$ can be found. The dashed contour lines are plotted using the approximate expressions for s_0 and $\mathcal{F}$, given by (33a) and (33b) and (45a) and (45b) in regions 2 and 3, respectively, and are almost indistinguishable from the actual values there.

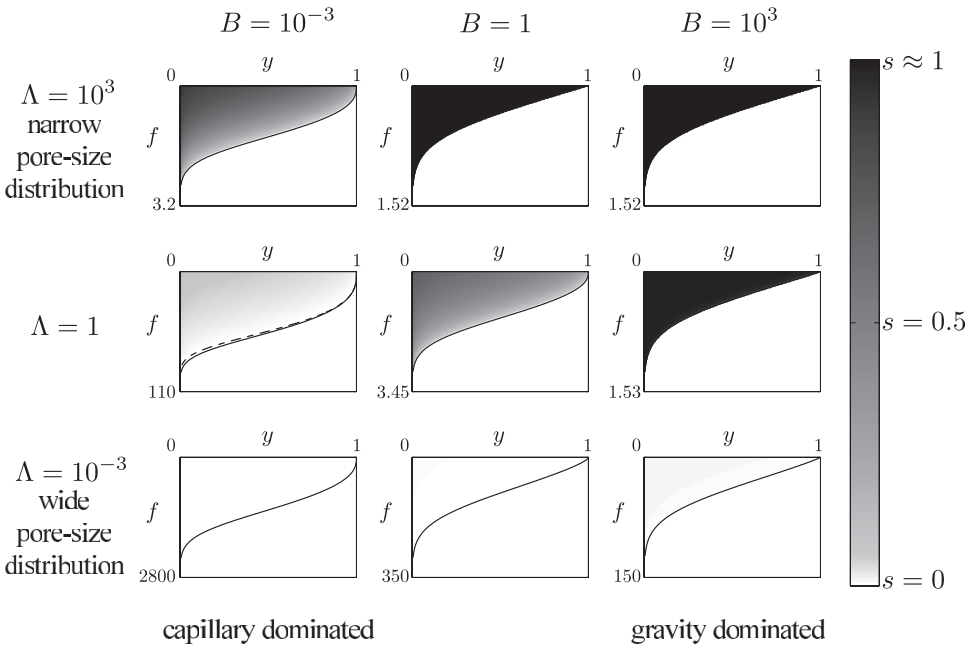

FIG. 3. Graphs demonstrating how the self-similar height profile of a two-phase gravity current, $f(y)$, varies with the strength of capillary forces. The gray shading indicates how the saturation distribution within the gravity current changes. Strengthening capillary forces, corresponding to decreasing B and Λ, lead to a thicker current, with a more rounded front and lower saturations. The dashed curve when $B = 10^{-3}$ and $\Lambda = 1$ shows the approximate profile in the limit of strong capillary forces, given by the solution of (40). The single-phase height profile predicted by Lyle *et al.*[1] is almost identical to the two-phase profile displayed for $B = 10^3$ and $\Lambda = 10^3$. Note the difference in vertical scale for each graph.

Figure 3 displays height profiles of the currents with parameter values $\Lambda = 10^{-3}$, 1, 10^3 and $B = 10^{-3}$, 1, 10^3, resulting from the numerical solution of (28)–(32). The main effect of increasing capillary forces, either by decreasing B or decreasing Λ, is to lower the saturation everywhere in the current. This leads to reduced relative permeability and in order to maintain a constant flux, the gradient of the current along the boundary, $\partial h/\partial r$, must increase. This effect is particularly significant near the front of the current where the height goes to zero and therefore leads to a blunter nose shape in two-phase currents. When capillary effects are strong, as discussed in Sec. IV B, the front of the current takes the shape $f \sim (1 - y)^{1/3}$, for example when $B = 10^{-3}$ and $\Lambda = 1$ in Figure 3. The thickness of the current is also increased due to the lower saturations for two reasons. First, mass conservation requires that for a given flux, the height must increase. Second, the reduced relative permeability may require a steeper gradient everywhere in the current, not just near the nose, for example, when $B = 1$ and $\Lambda = 10^{-3}$ in Figure 3. It is important to note that to return to dimensional heights, the profiles displayed in Figure 3 are multiplied by H, which for fixed h_e, scales with B.

Contour plots of the dimensionless height at $y = 0.5$ and the multiplicative factor η_N against B and Λ are displayed in Figures 4 and 5, respectively. The dimensionless current height, f, increases with increasing capillary forces due to mass conservation and reduced relative permeability because the average saturation within such currents decreases. The behaviour of f and η_N in terms of s_0 and $\mathcal{F}$ is given by the scaling relations (22) and (26). There are three parameter regimes in which we can use these scaling relations, along with the approximations of s_0 and $\mathcal{F}$, to find simple explicit expressions for how the dimensionless height and radius of the current scale in terms of the parameters B and Λ. The first regime corresponds to the case of negligible capillary forces, where the governing equations reduce to those for a single-phase gravity current. The second regime corresponds to when capillary forces are very strong, such that the saturation distribution is linear throughout the full vertical extent of the current. The third region corresponds to intermediate capillary forces, where the Bond number

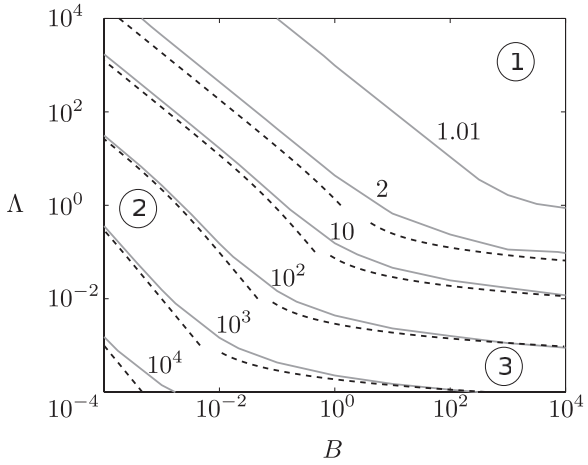

FIG. 4. Contour plot of the dimensionless current height, f, at $y = 0.5$, normalised by the corresponding height of a single-phase gravity current, $f_{SP}(0.5) = 0.348$, as a function of Λ and B. The solid curves indicate solutions of the full numerical equations. The circled numbers correspond to regions of (1) weak, (2) strong, and (3) intermediate capillary forces, discussed in Secs. IV A–IV C, respectively. The dashed curves depict the contours calculated using the approximations in regions of strong and intermediate capillary forces. These approximate contour lines have been calculated using constants of proportionality 1 in (38a) in region 2, and 0.5 in (47) in region 3.

is large but the capillary effects are augmented by a wide pore-size distribution. The three regimes are labelled 1, 2 and 3 in Figures 4 and 5.

The physical interpretation and analysis of the three regions in which approximate solutions can be found are discussed in Secs. IV A–IV C. For all other values of Λ and B, it is not possible to find approximate expressions for the saturation and flux functions, or height profile f, and full numerical solutions of (28) must be obtained. However, an indication of the orders of magnitude can be obtained from the contour plots shown in Figures 4 and 5.

A. Weak capillary forces

Capillary forces are negligible when the Bond number is relatively large, $B \gg 1/\Lambda$, indicating a low capillary entry pressure, and the pore-size distribution is narrow, $\Lambda \gg 1$. The saturation $s \approx 1$

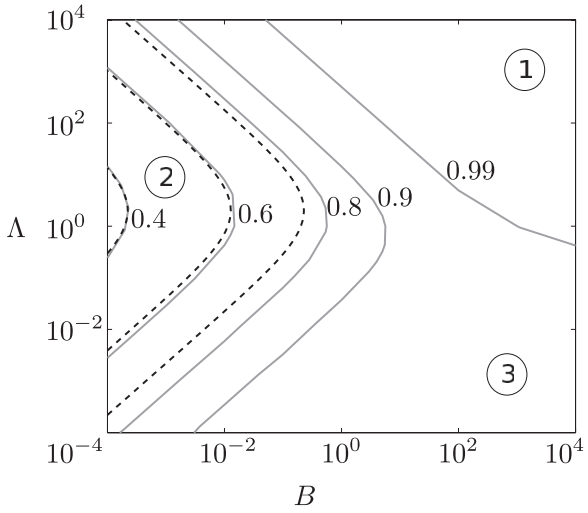

FIG. 5. Contour plot showing the variation of η_N/η_N^{SP} with Λ and B, where $\eta_N^{SP} = 1.155$ is the value in the single-phase limit. The circled numbers correspond to regions of (1) weak, (2) strong, and (3) intermediate capillary forces, discussed in Secs. IV A–IV C, respectively. In the limit of strong capillary forces, $\eta_N = 0.8704(2 + \Lambda)^{1/5}(B/\Lambda)^{1/10}$, as discussed in Sec. IV B. The contours using this approximation for $\eta_N/\eta_N^{SP} = 0.4$, 0.6, and 0.8 are shown by the dashed curves.

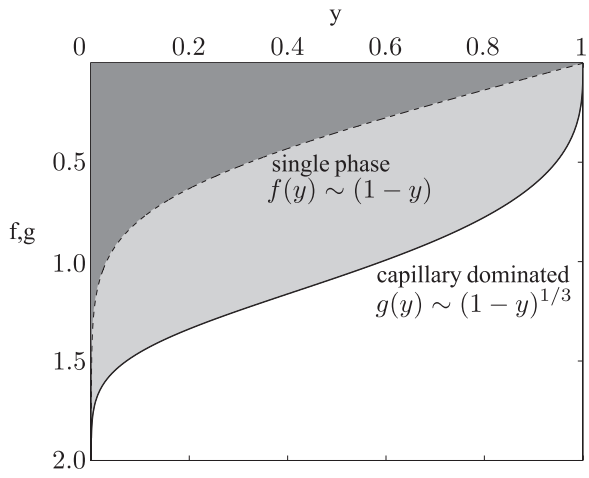

FIG. 6. Graph of the scaled current height profiles in various limits. The dashed curve shows $f(y)$ in the single-phase limit. The solid curve shows $g(y)$, in the limit of very strong capillary forces, where $f(y) = [\Lambda^2 B^3(2+\Lambda)]^{-1/5} g(y)$.

throughout most of the depth of the current, and hence the saturation and flux functions are closely approximated by

$$s_0 \approx 1 \tag{35a}$$

and

$$\mathcal{F} \approx 1. \tag{35b}$$

In this limit, the problem defined by (28)–(30) reduces to that of a single-phase gravity current derived by Lyle *et al.*,[1] where $\eta_N = \eta_N^{SP} = 1.155$ and the dimensionless height profile $f(y)$ is independent of Λ and B and has order of magnitude equal to one. The function $f(y)$ is plotted in Figure 6 and exhibits the characteristic shape of a single-phase gravity current.

B. Strong capillary forces

When capillary forces are very strong throughout the current, the distribution of the non-wetting phase saturation is approximately linear with depth,

$$s(f, z) \approx \Lambda B(f - z). \tag{36}$$

This occurs when the capillary pressure drop between $z = 0$ and $z = h$ is small. For this approximation to be valid everywhere, the second term in the Taylor expansion of $s(f, z)$ must be small, i.e.,

$$(\Lambda + 1) f B \ll 1. \tag{37}$$

If the pore-size distribution is very narrow, the Bond number must be very small to produce a linear saturation profile throughout the vertical extent of the current. When the pore-size distribution is very wide, capillary forces are strong, but the wide capillary fringe causes the current height to be very large. This can lead to the linear approximation for the saturation distribution not being appropriate near the base of the current, where s_0 is calculated, unless the Bond number is sufficiently small.

When the saturation distribution is linear throughout the height of the current, the saturation and flux functions are given by (33a) and (33b). As noted in Sec. III, these approximations are always true at the current nose. Contour plots using each approximation are shown by dashed lines in region 2 of Figures 2(a) and 2(b), and are mostly indiscernible from the actual values.

Substituting (33a) and (33b) into (26) and (22), we find that

$$f \sim [\Lambda^2 B^3(2+\Lambda)]^{-1/5} \tag{38a}$$

and

$$\eta_N \sim (2+\Lambda)^{1/5}\left(\frac{B}{\Lambda}\right)^{1/10}. \tag{38b}$$

The former is used to plot the dashed contour lines in the corresponding region of Figure 4. We can therefore re-cast our similarity solution in terms of

$$f(y) = [\Lambda^2 B^3(2+\Lambda)]^{-1/5} g(y) \tag{39a}$$

and

$$\eta_N = \hat{\eta}_N(2+\Lambda)^{1/5}\left(\frac{B}{\Lambda}\right)^{1/10}, \tag{39b}$$

for the case where (33a) and (33b) are valid throughout the current, where $g(y)$ and $\hat{\eta}_N$ are new order one variables. In this limit, the governing equations, (28) and (30), become independent of B and Λ and are given by

$$\left[y g^4 g'\right]' + \frac{1}{2}\hat{\eta}_N^2 y^2 g g' = 0 \tag{40}$$

and

$$\hat{\eta}_N = \left[\pi \int_0^1 g^2 y dy\right]^{-1/2}. \tag{41}$$

We calculate that $\hat{\eta}_N = 0.8704$ and dashed contour lines for η_N using (39b) are plotted in Figure 5. They show good agreement with the numerically obtained values in this strong capillary force limit. The function $g(y)$ is plotted in Figure 6 and the similarity height profile (39a) is plotted using a dashed curve in Figure 3 when $B = 10^{-3}$ and $\Lambda = 1$. Equation (40) indicates that the shape of the current when $1 - y \ll 1$ is $g \propto (1-y)^{1/3}$, which bears a resemblance to the profile of a viscous gravity current on a horizontal boundary near the nose of the current.[16]

We return to the condition for the validity of this approximation, and by substituting (38a) for the current height scale into (37), we find that the linear approximation is valid when

$$(\Lambda+1)(B/\Lambda)^{1/2} \ll 1. \tag{42}$$

Hence, this regime occurs when

$$B \ll 1 \qquad (\Lambda \sim 1), \tag{43a}$$

$$\Lambda B \ll 1 \qquad (\Lambda \gg 1), \tag{43b}$$

and

$$B/\Lambda \ll 1 \qquad (\Lambda \ll 1), \tag{43c}$$

which in all scenarios of pore-size distribution require the Bond number to be very small, indicating that capillary forces are very strong compared to gravity forces. We note that in these limits the saturation of the non-wetting phase in the current may be too small for the assumptions leading to gravity-capillary equilibrium to be valid. However the calculations do provide a limiting case for the behaviour of two-phase gravity currents where capillary forces are very strong.

C. Intermediate capillary forces with a wide pore-size distribution: $fB \gg 1$, $\Lambda \ll 1$

The effectiveness of capillary forces at creating a partially saturated zone is a function of both the Bond number and pore-size distribution. Thus, even moderate or weak capillary forces, where $fB \gg 1/\Lambda$ for most of the current, can result in a large capillary fringe as long as the pore-size distribution is sufficiently broad, $\Lambda \ll 1$. The presence of a wide capillary fringe thickens the current due to the lower average saturation. However, the lower capillary entry pressure indicated by a large

Bond number means that it is easier for the non-wetting phase to enter pores. Therefore, the profile of the current front approaches the linear shape observed in single-phase gravity currents.

In this regime, the saturation distribution is approximately

$$s(fB, z) \approx \Lambda \log[1 + B(f - z)], \tag{44}$$

and the saturation and flux functions can be approximated by

$$s_0(\Lambda, fB) \approx \Lambda \log(1 + fB) \tag{45a}$$

and

$$\mathcal{F}(\Lambda, fB) \approx \Lambda^2 \left[\log^2(1 + fB) - 2\log(1 + fB) + 2\right]. \tag{45b}$$

Contour lines using (45a) and (45b) are indicated by dashed curves in region 3 of Figures 2(a) and 2(b). This approximation for s_0 is in fact very good for all fB when $\Lambda \ll 1$.

We therefore know from substituting (45b) into (26) that in this regime, the dimensionless height scales as

$$f \sim 1/\Lambda[\log^2(1 + fB) - 2\log(1 + fB) + 2]^{1/2}. \tag{46}$$

Hence, to first approximation $f \sim 1/\Lambda$ and substitution of this back into the right-hand side of (46) yields

$$f \sim 1/\Lambda[\log^2(1 + B/\Lambda) - 2\log(1 + B/\Lambda) + 2]^{1/2}, \tag{47}$$

which is used to plot the dashed contour lines in the corresponding region of Figure 4. Similarly we find that to good approximation

$$\eta_N \sim \left[\frac{\log^2(1 + B/\Lambda) - 2\log(1 + B/\Lambda) + 2}{\log^2(1 + B/\Lambda)}\right]^{1/4}, \tag{48}$$

which does not differ greatly from unity as B/Λ is varied. This indicates that in this intermediate capillary force limit, the value of η_N is close to the single-phase limit. This is visualised in Figure 5, where all values of η_N/η_N^{SP} in the region of small Λ and large B are greater than 0.9.

Furthermore, we note that in this regime $\eta_N = \eta_N(B/\Lambda)$ and $f = \bar{g}(y, B/\Lambda)/\Lambda$ and so the quotient B/Λ becomes the only remaining parameter in determining the scaled, dimensionless height profile, $\bar{g}(y)$ and η_N when $\Lambda \ll 1$. The behaviour of s_0, $\mathcal{F}$, and f in this region, visualized in Figures 2 and 4, indicates that when the pore-size distribution is wide, capillary forces are important even as B becomes large.

V. APPLICATION TO THE CO_2 STORAGE SITE AT SLEIPNER

The theory presented has shown that the extent of an axisymmetric two-phase gravity current increases as $t^{1/2}$ and depends on the properties of the two fluids and the porous medium as described by (21). However, the properties of reservoir rocks, such as their permeability, pore-size distribution, and wetting properties, may be poorly known, or sampled with low spatial resolution. As we have shown, the rate and manner of fluid propagation can be affected by these properties and therefore it represents a sensitive probe of subsurface conditions. Furthermore, seismic images provide an excellent tool for mapping the subsurface flow of CO_2. Therefore, one useful application of this work is to exploit the dependence of observed fluid flows on relatively well-constrained fluid properties to infer rock characteristics, whilst quantitatively capturing the effects of capillary forces.

One of the most intensively studied CO_2 sequestration sites is the Sleipner project in the North Sea, where supercritical CO_2 has been injected into the Utsira sandstone formation since 1996 at a rate of $\sim$1 MT/yr. Seismic imaging has shown that the injected CO_2 has been advancing through the formation and is now spreading beneath nine relatively impermeable mudstone layers. Bickle *et al.*[20] measured the area covered by the CO_2 phase at each shale layer and calculated the equivalent radius of an axisymmetric current as a function of time. Estimates for the porosity of the formation

rock, as well as the viscosity and density of CO_2 and brine at each layer, are thought to be relatively well constrained. The areal extent of the current at each layer is observed to increase linearly in time, as is the case for the two-phase axisymmetric gravity current analysed in this paper, and its single-phase counterpart studied by Lyle *et al.*[1] Thus the predicted radial growth rate with respect to time is verified. A second useful application of the model is to make estimates of the more poorly constrained multiphase parameters. Bickle *et al.*[20] used the single phase axisymmetric model to estimate the flux into each layer. The intrinsic permeability of the rock, a quantity which is poorly known, was then implied to ensure conservation of the total mass of CO_2 injected into the formation, allowing for underestimates arising from fluid contained in parts of the current too thin to be detected by seismic imaging. They found a value of $k = 0.19 \pm 0.014 \times 10^{-12}$ m^2, which is approximately an order of magnitude smaller than the permeability, $k = 1.1 - 5 \times 10^{-12}$ m^2 ($1.1 - 5$ D), measured from a core sample of the same sandstone formation, some distance away from the injection site. Bickle *et al.*[20] proposed that this apparent discrepancy between predicted and measured permeabilities might be caused by the reduction in relative permeability due to capillary effects in the two-phase system, which are not captured by the sharp-interface model.

Here, we use the seismically observed areal extent of the gravity current at each layer within the Utsira formation, along with our prediction of the spreading of a two-phase gravity current given by (21). We take the parameter values for $\Delta\rho$ and μ_N at each layer and $\phi = 0.375$, as suggested by Bickle *et al.*,[20] and set $S_{wi} = 0.05$ and $k_{rn0} = 1$, as estimated by Chadwick, Noy, and Holloway.[21] The Brooks-Corey capillary entry pressure parameter, p_e, and pore-size distribution parameter, Λ, are harder to determine. We use a value of $\Lambda = 2/3$, converted from the van Genuchten model for capillary pressure used by Chadwick, Noy, and Holloway[21] for the Sleipner storage site. Representative estimates for permeability obtained from core samples and well-test data in Bickle *et al.*[20] are $k = 1.1 \times 10^{-12}$ m^2, 3×10^{-12} m^2, and 5×10^{-12} m^2 and we suppose that these values are representative of the Sleipner storage site. For each of these values, we imply the capillary entry pressure that ensures the total flux 1 MT/yr is conserved among the 9 layers. In doing so, we infer that $p_e = 2 \times 10^3$ k Pa, 2×10^4 k Pa, and 6×10^4 k Pa, respectively. Estimates in the literature for capillary entry pressure in the Utsira sandstone range from $p_e = 0.81$ k Pa, obtained experimentally from core samples,[22] to $p_e = 4$ k Pa, used in the reservoir simulator TOUGH2.[21] Therefore, the assertion that capillary effects may account for the observed rates of propagation cannot be reconciled with estimates for the capillary entry pressure within the Utsira sandstone, because this would require a capillary entry pressure that is 3–4 orders of magnitude larger than estimated, due to the small power of p_e in (21). We conjecture that the disagreement between models and observations might be explained instead by leakage that occurs between each thin shale layer as the CO_2 rises through the formation. This may cause the apparent flux into, and out of, each layer to vary in time, producing the observed temporal behaviour of the areal extent of the gravity currents. Evidence supporting this has been obtained from the latest seismic imaging survey of the Sleipner storage site, which is presented by Boait *et al.*[23] along with in-depth discussion about how the CO_2 is thought to be moving within the formation.

VI. DISCUSSION AND CONCLUSIONS

The most striking result of this study is that a two-phase axisymmetric gravity current, fed by a constant flux, propagates in a porous medium like $t^{1/2}$ in a self-similar manner. The extent therefore has the same time dependence as a single-phase axisymmetric gravity current, where capillary forces do not play a role.[1] The effects of capillary forces on the form and rate of propagation are incorporated in the gravity current model by saturation and flux functions. These two functions depend only on the Bond number B and the pore-size distribution parameter Λ. These factors are therefore the sole determinants of the rate of propagation, given by $r_N = \eta_N(B, \Lambda)t^{1/2}$, and the shape of the current.

Further comparison with a single-phase current provides insight into the way the dimensionless radius and height of the two-phase current scale with the strength of capillary forces, as given by (22) and (26). The radius and height of a single-phase current depend on the intrinsic permeability,

k, and porosity, ϕ, of the porous medium, according to

$$r_N \sim (k/\phi^2)^{1/4} \tag{49a}$$

and

$$h \sim k^{-1/2}. \tag{49b}$$

The main effect introduced by capillary forces is to reduce the saturation of the fluid within the current and this has two main consequences. First, the volume of fluid contained per unit horizontal area in the current is reduced, which is encapsulated by the saturation function $s_0(fB, \Lambda)$. Second, the relative permeability of the fluid in the current is reduced, which is captured by the flux function $\mathcal{F}(fB, \Lambda)$. The saturation and flux functions can therefore be interpreted as an effective porosity and an effective permeability, respectively, for the partially saturated non-wetting phase in the current. In addition, capillary forces introduce the existence of an irreducible wetting phase saturation and an endpoint relative permeability, which affect both the effective porosity and permeability of the porous medium. Thus the parallel comparison drawn between the two-phase effects on porosity and permeability and (49a) and (49b) explains the scaling in (19a) and (19b) of

$$r_N \sim \left[k_{rn0}\mathcal{F}/(1 - S_{wi})^2 s_0^2\right]^{1/4} \tag{50a}$$

and

$$h \sim (k_{rn0}\mathcal{F})^{-1/2}. \tag{50b}$$

Capillary effects also have a large influence on the shape and the thickness of two-phase gravity currents. Stronger capillary forces lead to lower saturation of the injected fluid and therefore lower relative permeability. The gradient of the current height profile consequently needs to be steeper in order to drive flow and maintain a given flux, which results in a thicker current. The capillary entry pressure determines how easily the non-wetting phase can advance into pores at the front of the current. The front of the current becomes rounded when the capillary entry pressure is high, or Bond number is low, in order that the height is sufficient to overcome the pressure threshold.

Residual trapping is one of the key mechanisms through which CO_2 may be immobilized during CO_2 sequestration. It occurs once injection has ceased. The two key factors determining the amount of the non-wetting fluid that is trapped are the saturation distribution at the onset of imbibition and the volume of rock reached by the CO_2, both of which are calculated by this two-phase model. The relation between initial and residual saturation of the non-wetting fluid for a given fluid-rock system must be obtained empirically, and is commonly summarized by a trapping model. Golding *et al.*[11] discussed in detail how a constant-flux drainage model can be used, in combination with a trapping model, to provide estimates of how much non-wetting fluid would be trapped in the wake of a two-dimensional, two-phase gravity current. In an analogous way, the axisymmetric model here provides the tool to obtain more accurate estimates of residual trapping in storage sites, such as Sleipner, where currents are spreading in a very approximately axisymmetric way.

In conclusion, we have presented a model that provides a way of quantitatively assessing how capillary forces affect the behaviour of an axisymmetric, constant-flux, two-phase gravity current as it propagates in a porous medium. It can be applied directly to data and observations on the reservoir scale in order to give estimates of the properties of the rock-fluid system, as demonstrated. Given the ill-constrained characterisation of the subsurface, the model provides a simple and invaluable way of exploring the sensitivity of predictions for two-phase gravity currents on parameter estimates, without the need to run a multitude of potentially costly numerical simulations. The model is also useful for obtaining quantitative estimates of the amount of residual trapping that would occur once injection has ceased, as discussed by Golding *et al.*[11] The theory presented here represents a significant advance in our understanding of how capillary effects, such as relative permeability, affect the propagation of two-phase, constant-flux gravity currents propagating axisymmetrically in porous media. Future work in preparation will incorporate drainage and imbibition consistently into a model for a two-phase gravity current resulting from a finite volume release, where the maximum height decreases with time and therefore capillary effects become increasingly more important.

ACKNOWLEDGMENTS

The research of M.J.G. is funded by the EPSRC, H.E.H. by a Royal Society Wolfson Merit Award, and J.A.N. is supported by a Royal Society University Research Fellowship. We would like to thank the reviewers for their time and for providing constructive comments to help us improve this paper.

APPENDIX: ALGEBRAIC EXPRESSION FOR $\mathcal{F}$

The definition of the flux function, (32), can be integrated analytically using integration by parts, which yields the expression

$$fB\mathcal{F} = \mathcal{F}^* + \frac{(1-s_0)^{(\Lambda+1)/\Lambda}}{3\Lambda+1}\left[s_0^2 + \frac{2\Lambda}{2\Lambda+1}s_0\right] + \frac{2\Lambda^2\left[(1-s_0)^{(\Lambda+1)/\Lambda}-1\right]}{(\Lambda+1)(2\Lambda+1)(3\Lambda+1)}, \tag{A1}$$

where

$$\mathcal{F}^*(fB) = \begin{cases} 1+fB-4(1+fB)^{1/2}+3+\log(1+fB) & (\Lambda = 1/2) \\ 1+fB-(1+fB)^{-1}-2\log(1+fB) & (\Lambda = 1) \\ 1+fB+\frac{1}{1-2\Lambda}(1+fB)^{1-2\Lambda}+\frac{2}{\Lambda-1}(1+fB)^{1-\Lambda}+\frac{2\Lambda^2}{(\Lambda-1)(1-2\Lambda)} & (\Lambda \neq 1/2, 1). \end{cases} \tag{A2}$$

[1] S. Lyle, H. E. Huppert, M. Hallworth, M. Bickle, and A. Chadwick, "Axisymmetric gravity currents in a porous medium," J. Fluid Mech. **543**, 293–302 (2005).
[2] D. Vella and H. E. Huppert, "Gravity currents in a porous medium at an inclined plane," J. Fluid Mech. **555**, 353–362 (2006).
[3] I. N. Kochina, N. N. Mikhailov, and M. V. Filinov, "Groundwater mound damping," Int. J. Eng. Sci. **21**(4), 413–421 (1983).
[4] M. A. Hesse, F. M. Orr, Jr., and H. A. Tchelepi, "Gravity currents with residual trapping," J. Fluid Mech. **611**, 35–60 (2008).
[5] R. Juanes, C. W. MacMinn, and M. L. Szulczewski, "The footprint of the CO_2 plume during carbon dioxide storage in saline aquifers: Storage efficiency for capillary trapping at the basin scale," Transp. Porous Media **82**, 19–30 (2010).
[6] J. Bear and V. Ryzhik, "On the displacement of NAPL lenses and plumes in a phreatic aquifer," Transp. Porous Media **33**, 227–255 (1998).
[7] M. Blunt, D. Zhou, and D. Fenwick, "Three-phase flow and gravity drainage in porous media," Transp. Porous Media **20**, 77–103 (1995).
[8] Y. C. Yortsos, "A theoretical analysis of vertical flow equilibrium," Transp. Porous Media **18**(2), 107–129 (1995).
[9] J. R. Philip, "Theory of infiltration," Adv. Hydrosci. **5**, 215–296 (1969).
[10] J. M. Nordbotten and H. K. Dahle, "Impact of the capillary fringe in vertically integrated models for CO_2 storage," Water Resour. Res. **47**, W02537, doi:10.1029/2009WR008958 (2011).
[11] M. J. Golding, J. A. Neufeld, M. A. Hesse, and H. E. Huppert, "Two-phase gravity currents in porous media," J. Fluid Mech. **678**, 248–270 (2011).
[12] C. S. Land, "Calculation of imbibition relative permeability for two- and three-phase flow from rock properties," Soc. Pet. Eng. J. **8**(2), 149–156 (1968).
[13] R. H. Brooks and A. T. Corey, "Hydraulic properties of porous media," *Hydrology Papers* (Colorado State University, 1964), Vol. 3.
[14] R. H. Brooks and A. T. Corey, "Properties of porous media affecting fluid flow," J. Irrig. and Drain. Div. **6**, 61 (1966).
[15] K. Li and R. N. Horne, "Comparison of methods to calculate relative permeability from capillary pressure in consolidated water-wet porous media," Water Resour. Res. **42**, W06405, doi:10.1029/2005WR004482 (2006).
[16] H. E. Huppert, "The propagation of two-dimensional and axisymmetric viscous gravity currents over a rigid horizontal surface," J. Fluid Mech. **121**, 43–58 (1982).
[17] H. E. Huppert and A. W. Woods, "Gravity-driven flows in porous layers," J. Fluid Mech. **292**, 55–69 (1995).
[18] I. Engelhardt, S. Finsterle, and C. Hofstee, "Experimental and numerical investigation of flow phenomena in nonisothermal, variably saturated bentonite-crushed rock mixtures," Vadose Zone J. **2**, 239–246 (2003).
[19] S. Bachu and D. B. Bennion, "Interfacial tension between CO_2, freshwater, and brine in the range of pressure from (2 to 27) MPa, temperature from (20 to 125) °C, and water salinity from (0 to 334 000) mg L^{-1}," J. Chem. Eng. Data **54**, 765–775 (2009).
[20] M. Bickle, A. Chadwick, H. E. Huppert, M. Hallworth, and S. Lyle, "Modelling carbon dioxide accumulation at Sleipner: Implications for underground carbon storage," Earth Planet. Sci. Lett. **255**, 164–176 (2007).

[21] R. A. Chadwick, D. J. Noy, and S. Holloway, "Flow processes and pressure evolution in aquifers during the injection of supercritical CO_2 as a greenhouse gas mitigation measure," Pet. Geosci. **15**, 59–73 (2009).
[22] R. A. Chadwick, R. Arts, and O. Eiken, "4D seismic quantification of a growing CO_2 plume at Sleipner, North Sea," in *Petroleum Geology: North-West Europe and Global Perspectives - Proceedings of the 6th Petroleum Geology Conference*, edited by A. Doré and B. Vining (Geological Society, London, 2005), pp. 1385–1399.
[23] F. C. Boait, N. J. White, M. J. Bickle, R. A. Chadwick, J. A. Neufeld, and H. E. Huppert, "Spatial and temporal evolution of injected CO_2 at the Sleipner Field, North Sea," J. Geophys. Res. **117**, B03309, doi:10.1029/2011JB008603 (2012).